



Segmenting cryo-electron tomography data: Extracting models from cellular landscapes

Danielle A. Grotjahn

Cryo-electron tomography provides an unprecedented view of cellular architecture, yet extracting meaningful biological insights remains challenging. Segmentation is a crucial step in this process through its ability to identify structural relationships between subcellular components visible in cryo-electron tomography data. While segmentation pipelines were historically low throughput, recent advancements in deep learning have significantly improved their automation, accuracy, and scalability. This review explores how these innovations redefine best practices for segmentation and accelerate biological discovery. This article highlights the critical role of segmentation in unlocking the full potential of cryo-electron tomography—not only for resolving macromolecular structures but also for quantifying their impact on subcellular organization and function.

Addresses

Department of Integrative Structural and Computation Biology, The Scripps Research Institute, 10550 North Torrey Pines Road, La Jolla, CA 92037, USA

Corresponding author: Grotjahn, Danielle A. (grotjahn@scripps.edu)

Current Opinion in Structural Biology 2025, **93**:103114

This review comes from a themed issue on **Cryo-electron microscopy (2024)**

Edited by **Pilar Cossio** and **Edward H Egelman**

For a complete overview see the [Issue](#) and the [Editorial](#)

Available online xxx

<https://doi.org/10.1016/j.sbi.2025.103114>

0959-440X/© 2025 The Author(s). Published by Elsevier Ltd. This is an open access article under the CC BY-NC-ND license (<http://creativecommons.org/licenses/by-nc-nd/4.0/>).

Introduction

Cryo-electron tomography (cryo-ET) has experienced a meteoric rise in popularity as a tool for visualizing organellar and macromolecular structures. While throughput in sample preparation and data collection has improved significantly, transforming the three-dimensional reconstructions (i.e. tomograms) into meaningful biological insights remains a significant hurdle. Just as atomic model building is key in single-particle cryo-electron microscopy (cryo-EM), segmentation is essential for turning tomographic data into

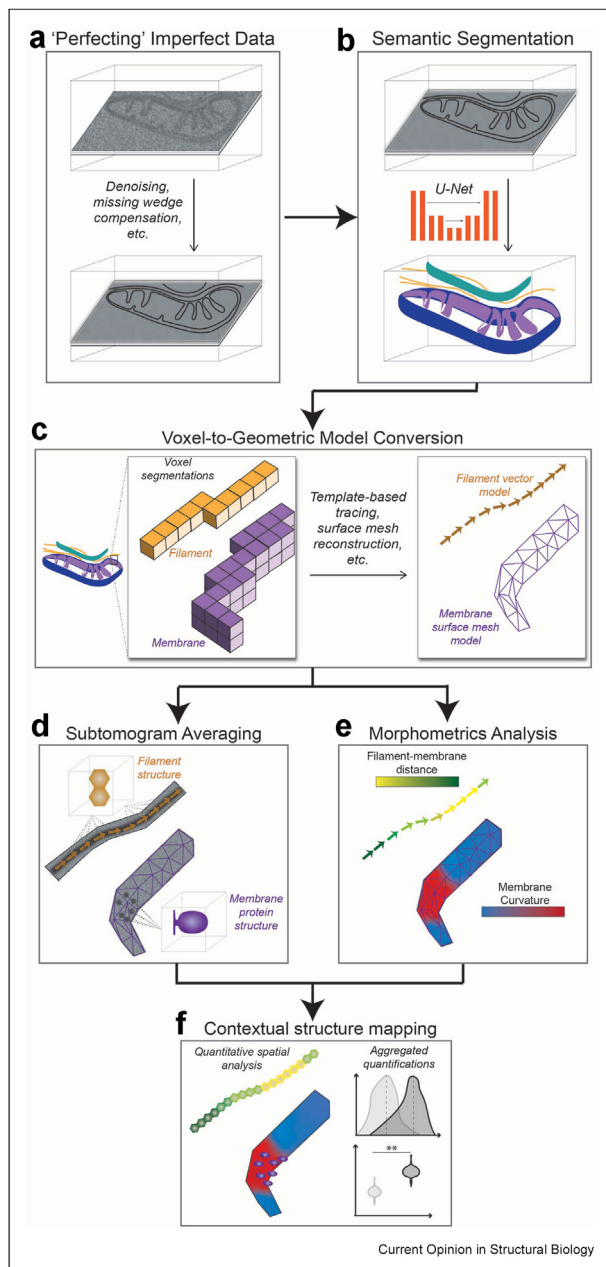
meaningful structural insights. Segmentation involves labeling each voxel in the tomogram according to its associated subcellular feature. The resulting segmentations not only reveal complex spatial relationships in three dimensions but, importantly, can serve as starting points for nearly all downstream analyses in cryo-ET, including subtomogram averaging and quantitative ultrastructural analyses (i.e. morphometrics). Historically, segmentation was a time-consuming, laborious process, typically reserved for a few ‘figure-worthy’ representative tomograms. The application of convolutional neural networks, particularly the U-net architecture [1], has automated segmentation to the point where we can think about it not as a ‘beautification’ technique but as a routine part of the processing workflow. This review will describe the modernization of segmentation workflows and demonstrate how they are essential for unlocking the full potential of cryo-ET for cellular structural biology (Figure 1).

‘Perfecting’ imperfect data is the first step toward automated segmentation

One of the first challenges in automating segmentation for cryo-ET data is that the input is inherently imperfect. The most apparent imperfection is the low signal-to-noise ratio (SNR) due to the low-dose imaging parameters required for imaging radiation-sensitive vitrified biological material, which makes segmentation challenging. Software like cryo-CARE [2], WARP [3], and Topaz [4] build noise models using the noise2noise algorithm [5]. By comparing the data to itself, conceptually similar to how half-map comparisons in single-particle cryo-EM help isolate true signal, these noise models learn to distinguish signal from noise in the raw tomograms. Denoising algorithms suppress the high-frequency noise while preserving structural detail, resulting in tomograms with enhanced contrast that improve automated downstream segmentation tasks.

One drawback of these approaches is that increased image contrast often comes at the cost of potentially suppressing ‘real’ high-frequency structural information. The recently released CryoSamba [6] denoising software differs from other approaches by leveraging neighboring slices within the tomogram to train the network to distinguish consistent signal from random noise. These results in improved contrast in tomograms

Figure 1



Modern segmentation workflows streamline downstream analysis of macromolecular and organellar structure from cryo-ET data. (a) 'Perfecting' imperfect tomographic data by applying algorithms designed to boost signal-to-noise is a common first step in automated segmentation pipelines. (b) The application of deep learning, particularly the U-net architecture, facilitates automated semantic segmentation of multiple organellar feature classes (i.e. membranes and filaments) from cryo-electron tomography data. (c) Transforming voxel segmentations into geometric models is a critical step for downstream data analysis. (d) Geometric models of filaments and membranes facilitate subtomogram averaging by providing *a priori* information about an associated macromolecule's location and orientation. (e) Geometric models enable the quantification of organellar ultrastructure through morphometrics analysis. (f) Segmentation-guided contextual structure mapping quantitatively reveals the spatial relationship between macromolecular structures and their local subcellular environment. cryo-ET, cryo-electron tomography.

with less aggressive suppression of high-frequency structural information compared to other denoising approaches. While most segmentation workflows to date have been performed in heavily binned data, typically at 10–20 Å pixel sizes, recent improvements with Cryo-Samba suggest a future shift toward using unbinned data (2–3 Å) for segmentation. This could enable segmentation itself to capture high-frequency variations in cellular ultrastructure that more faithfully reflect the true underlying biological signal.

Aside from low SNR, tomographic data also suffers from artifacts due to incomplete sampling that distort cellular structures, causing spurious or inaccurate segmentation in some areas of the tomogram. The 'missing wedge' is an artifact that arises from the limited tilt range during collection due to the physical constraints of the microscope. Isonet [7] and DeepDeWedge [8] both harness deep learning to recover the 'missing wedge' and perform image denoising on tomographic data. Cryo-TIGER [9] uses deep learning to recover information lost due to discrete tilt angle sampling during data collection, and initial benchmarking demonstrates that this can improve membrane segmentation. While it is easy to get caught up in finding the optimal data 'perfection' approach, we have found that applying any of the software mentioned above can improve segmentation accuracy over unprocessed data. Therefore, in practice, I recommend prioritizing a strategy that balances ease of use, automation, and accuracy for your segmentation workflow (Figure 1a).

The U-Net architecture revolutionized the semantic segmentation of cryo-ET data

Traditionally, feature localization (i.e. particle picking) and segmentation were treated as distinct tasks in cryo-ET workflows, with localization focusing on identifying individual macromolecules and segmentation providing labels for cellular ultrastructure. However, the development of the U-net-based approaches [11] has blurred this distinction, as these methods have proven successful at both labeling subcellular features and detecting macromolecular complexes simultaneously (Figure 1b). Beyond label assignment, segmentation outputs can be leveraged as 'masks' to filter false positives from template matching, including for cytosolic proteins. This exemplifies how prioritizing segmentation early in the workflow can enhance the specificity and efficiency of downstream processing tasks.

EMAN2 [10] was the first U-Net-based cryo-ET segmentation software and involved manually tracing pixels within 2D slices for training. Nearly four years passed before the release of DeepFinder [11], the first fully supervised 3D U-Net for tomographic segmentation. Shortly after, the multislice U-Net in Dragonfly [12] was

adapted to cryo-ET data, enabling the automatic segmentation of multiple feature classes simultaneously. A significant roadblock in deep learning-based approaches for segmentation is the lack of ground truth data and/or pretrained models that can be applied broadly across different cryo-ET datasets. DeepPict [13] is the first segmentation tool to offer a pretrained model on a large dataset of expert-annotated tomograms from cryo-FIB (focused ion beam)-milled yeast lamellae. Recently, several groups have attempted to address the ground truth challenge by generating simulated datasets in which atomic or geometric models of filaments or membranes are computationally degraded to mimic artifacts inherent to tomographic reconstruction. These studies demonstrate that simulated data can be used to train U-net models for the semantic segmentation of real cryo-ET datasets [14–16]. These efforts point to a promising future where tomogram-like simulations could be used to train generalizable segmentation models across a wide range of structures, including those deposited in the Protein Data Bank (PDB).

Due to their sensitivity to artifacts from dehydration and chemical fixatives, cellular membranes are a common target for cryo-ET imaging, driving significant efforts to develop automated analysis approaches tailored to them. For nearly a decade, TomoSegMemTV [17] represented the state-of-the-art software for automated segmentation of membranes from tomographic data. However, achieving optimal performance requires fine-tuning many parameters and manual cleanup in software like Amira [18] or Colabseg [19]. Curated datasets from TomoSegMemTV outputs were recently used to generate training data for developing a robust U-net-based approach, MemBrain v2 [20], which has become the new gold standard in automated membrane segmentation. As an alternative to generalized tools, CryoVesNet [21] offers a tailored solution to researchers investigating synaptic vesicles. Many of these membrane-specific workflows are organelle-agnostic, requiring an additional step—often requiring the eye of an expert microscopist—to label membranes associated with specific organelles.

Transforming voxel segmentations to geometric models is critical for downstream analysis

Automated machine learning (ML)-based segmentations typically assign labels to voxels, which produce jagged approximations of organelle structures, a problem worsened when applied to binned tomograms. Voxel spacing also dictates the resolution of resulting measurements, and slight imperfections in segmentations can result in potentially pixel-dependent differences in ultrastructural quantifications. For these reasons, converting voxel-based segmentation into vectors or triangle meshes provides a more continuous and mathematically defined

representation of structures that is ideal for downstream structural analysis (Figure 1c).

Surface mesh models represent a membrane as a continuous plane partitioned into vertices and polygons independent of pixel size. Pycurv [22] was the first program that performed this transformation on segmentations from cryo-ET data, enabling the calculation of membrane features such as surface normals and curvature. This approach worked well for simple sphere membrane segmentations but performed suboptimally for more complex, highly pleomorphic membrane segmentations. In these cases, the workaround was to generate a manual ‘in-painted’ volume segmentation such that the segmentation itself is the membrane and the luminal space in between. This requires significant user intervention and becomes more complicated because complex membranes, such as inner mitochondrial membrane cristae, do not often contain a clear ‘inside’ or ‘outside.’ To tackle this challenge, we developed a workflow that converts voxel segmentations into oriented point clouds that can be transformed into surface meshes using a screened Poisson surface reconstruction algorithm [23].

For filaments, the best strategies to generate geometric models for downstream analysis used template-based correlation to generate vectors representing the filament’s central line [24–26]. The fiber tracing module in Amira incorporates these algorithms and is a popular method for labs with access to this software. A major limitation of these correlation-based methods is that they often result in many false positives that must be manually curated. Streamlined workflows harness deep learning approaches such as Dragonfly or DeePiCt as a first-pass detection of different filamentous assemblies in cellular tomograms, followed by tracing of the binary segmentation output using the Xfiber module in Amira [15,27,28]. This process can also be iterated to maximize both training and model generation efficiency [28].

Segmentation guides subtomogram averaging

The artifacts and low SNR of tomograms make computationally identifying and aligning individual macromolecules through subtomogram averaging difficult. These challenges have historically been remedied using geometric models to provide *a priori* information about a macromolecule’s location and orientation within the tomogram [29–31]. However, most models must be generated manually. A workaround is to convert the models generated through automated segmentation into file formats (i.e. tables) that can be read and processed by programs like Dynamo [26,28,32] (Figure 1d), a pipeline streamlined thanks to the collaborative online platform [33] <https://teamtomo.org/>.

While geometric information can help identification, strong signals from membranes and filaments can paradoxically complicate alignment. One clever strategy used the membrane segmentation to dampen the membrane signal before particle extraction [34]. The authors note that this membrane signal suppression strategy was essential for resolving the α -amino-3-hydroxy-5-methyl-4-isoxazolepropionic acid (AMPA) receptor on neuronal synapses, offering an alternative to traditional parameter optimization and masking-based approaches in subtomogram averaging workflows.

Segmentation quantifies organelle shape through morphometric analyses

While other volumetric EM methods may excel at surveying larger cell volumes, cryo-ET provides significant benefits in resolution to glean subtle, albeit often functionally relevant, differences in subcellular architecture. Substantial advances in automated cryo-FIB milling [35] now facilitate the routine generation of dozens of lamellae with minimal manual intervention, transforming a technique with a dismally low throughput into arguably one of the highest-resolution cell biology approaches available for the quantitative analysis of ultrastructure (i.e. morphometrics) (Figure 1e). Mitochondria are a popular target for morphometrics analysis, and segmented models have been used to quantify the architecture of mitochondrial constriction sites [36,37], the changes that occur to mitochondrial cristae upon disease pathology [38], or in response to genetic manipulation of key cristae remodelers [39]. We recently developed a ‘surface morphometrics pipeline’ [23] to streamline the ultrastructural quantification of several membrane parameters relevant to organellar function, including membrane distance, curvature, and orientation. This pipeline has been used to investigate the remodeling of mitochondria [23,40], the endoplasmic reticulum [41], autophagosomes [42], the nuclear envelope [43,44], the plasma membrane [45], and viral replication vesicles [46]. Similar morphometrics approaches are available to analyze filaments [47] and have been recently applied to generate mechanistic models for the role of actin filaments during glucose-stimulated insulin secretion [48], neuronal growth cone formation [27,49], and plasma membrane mechanics [50].

Segmentation models can be used to quantitatively analyze the voxel intensity values within the tomogram. This analysis can produce a ‘map’ of densities within a fixed distance of the membranes, facilitating interactive or automated identification of membrane-associated proteins [20,51]. Segmentation-guided density analysis is also extensively used to identify associated densities radiating from synaptic vesicles [52–54]. We and others have used segmentation and surface mesh models to

perform local density sampling to measure membrane thickness, revealing local variations in bilayer thickness across organelles [46,55,56].

Segmentation contextualizes macromolecular structure with subcellular environment

The most powerful application of cryo-ET is its ability to not only resolve structures but also quantitatively assess how these structures influence and are influenced by the local subcellular architecture (Figure 1F). We recently used our surface mesh models to identify and subsequently solve the structure of cytoplasmic ribosomes likely engaged in co-translational protein import [57] (Figure 2a). We then isolated the ‘patches’ of triangles within the surface mesh closest to these import-primed ribosomes and demonstrated that the distance between the outer and inner membrane at these regions is significantly reduced relative to the other parts of the membrane (Figure 2b). Another group used a similar segmentation-guided strategy to solve the structure and organization of a different population of cytoplasmic ribosomes—those that use the mitochondrial outer membrane as a scaffold to ‘hibernate’ to prevent translation during glucose depletion [58]. Segmentation-guided contextual structure mapping approaches have also revealed the Ebola virus nucleocapsid assembly process [32], the life cycle of apicomplexan parasites [59,60], and storage mechanisms utilized by mammalian oocytes that enable mammalian development [61].

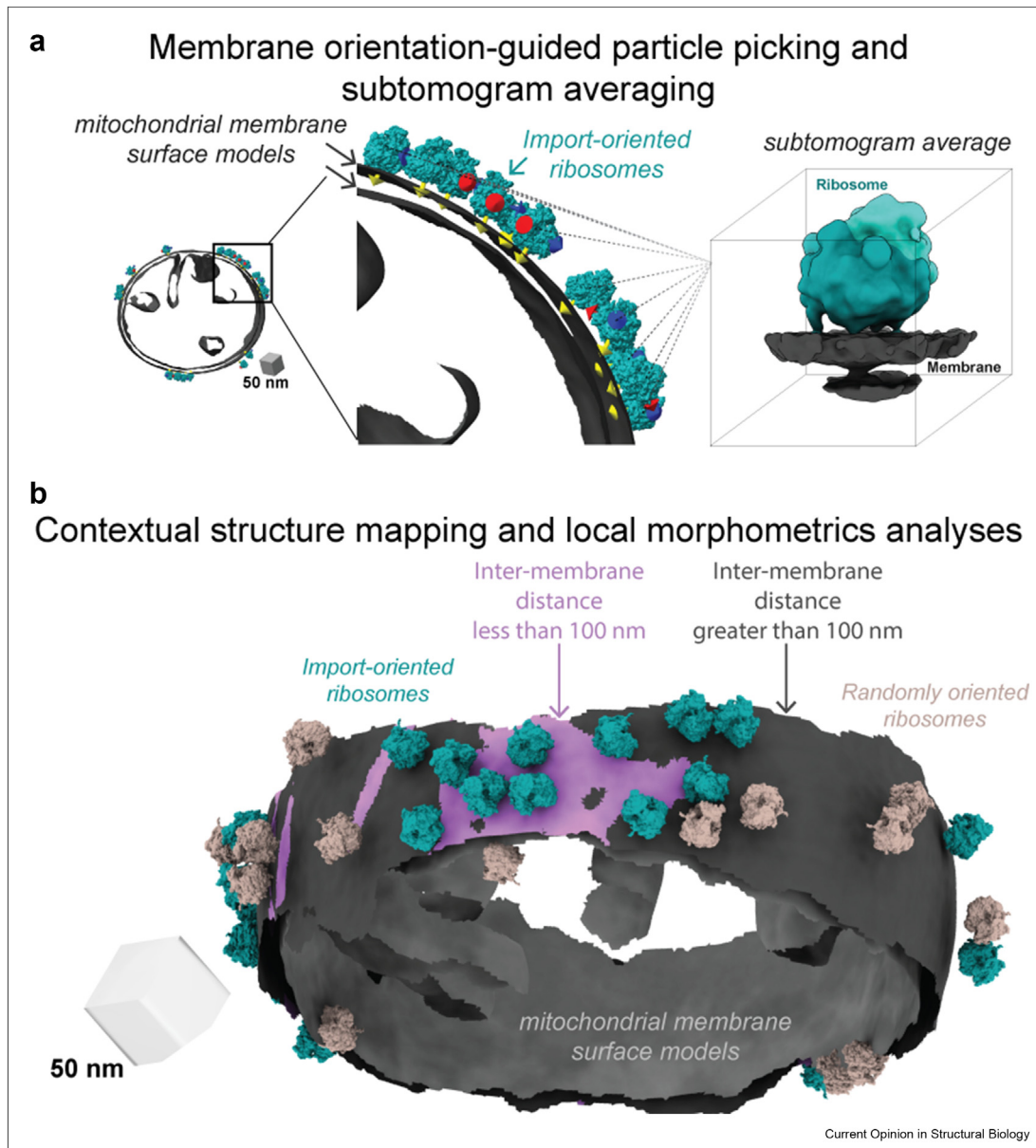
Three-dimensional model visualization hides the noise of tomographic data

Communicating complex three-dimensional information to the scientific community is equally important as generating and processing the segmented models with downstream analysis approaches. Several ML-based automated segmentation software, including EMAN2 [10], DeepPiCt [13], and Dragonfly [12], have graphical user interfaces (GUIs) for visualizing the resulting output semantic segmentations. Software like Amira [18], blik [62], Blender [63], Surforama [51], and ArtiaX [64] can simultaneously render segmentations and 3D geometric models directly overlaid on the tomographic volumes. ParaView [65] and PyVista [66] enable visualization of the morphometrics quantifications on the surface mesh reconstructions, highlighting local changes in ultrastructure.

Reconstructing the future of segmentation

Segmentation is the gateway to almost every downstream analysis and should, therefore, be prioritized in modern cryo-ET processing pipelines. Automation must be balanced with the ability to customize to a given project, and current efforts to streamline these steps are promising [67,68]. Increased automation hopefully means

Figure 2



Surface mesh-guided subtomogram averaging and structure mapping analysis. (a) Import-oriented ribosomes were identified by selecting ribosomes (cyan) with their peptide exit tunnel (yellow arrow) pointed toward the mitochondrial membrane surface model (dark gray). This process was repeated for all ribosomes in the dataset to produce a subtomogram average structure of a cytoplasmic ribosome oriented for import at the mitochondrial membrane. (b) Local 'patch'-based membrane surface mesh analysis identified clusters of import-oriented ribosomes associated with reduced outer-to-inner mitochondrial membrane (i.e. intermembrane) distances relative to randomly oriented ribosomes (tan) at the mitochondria surface. This figure is generated from data associated with EMD-48751 [57].

more ground truth data, as impressively demonstrated by the developers of Ais [67] and TARDIS [68], who used their approach to segment over ten thousand tomograms from the Chan Zuckerberg Initiative (CZI) cryo-ET data portal [69]. As automated segmentation becomes a household name in cryo-ET workflows, the field will soon need to develop deposition standards and validation metrics—an area currently under development [70].

Standardizing the deposition of models and their corresponding morphometrics alongside sample information (i.e. genotype or chemical perturbation) could potentially enable mathematical modeling that incorporates complementary data on kinetics, forces, and dynamics. This paves the way for a future where segmentations are transformed into molecular movies that bring static cryo-ET images to life.

Declaration of generative AI in scientific writing

While preparing this work, the author used ChatGPT4.0 and Grammarly to improve writing clarity and conciseness.

Funding sources

Danielle Grotjahn is supported by the Nadia's Gift Foundation Innovator Award of the Damon Runyon Cancer Foundation (DRR-65-21), the National Institutes of Health (NIH) grant (RF1NS125674), The Pew Scholars Program in the Biomedical Sciences, The Bachrach Family Foundation, The Donald E. and Delia B. Baxter Foundation, The Chan Zuckerberg Initiative (NS-CS-0000000010), and Scripps Research start-up funds.

Declaration of competing interest

The authors declare that they have no known competing financial interests or personal relationships that could have appeared to influence the work reported in this paper.

Acknowledgements

Thanks to Ben Barad for his input on the manuscript and for being a steadfast ally on our shared journey through segmentation and morphometrics. Thanks to Atty Chang for help with figures. I apologize for any omissions of recent work due to text limitations.

Data availability

No data was used for the research described in the article.

References

Papers of particular interest, published within the period of review, have been highlighted as:

- * of special interest
- ** of outstanding interest

1. Ronneberger O, Fischer P, Brox T: **U-Net: convolutional networks for biomedical image segmentation**. 2015.
2. Buchholz TO, Jordan M, Pigino G, Jug F: **Cryo-CARE: content-aware image restoration for cryo-transmission electron microscopy data**. In *2019 IEEE 16th international symposium on biomedical imaging (ISBI 2019) 8-11 april 2019*; 2019: 502–506.
3. Tegunov D, Cramer P: **Real-time cryo-electron microscopy data preprocessing with Warp**. *Nat Methods* 2019, **16**: 1146–1152.
4. Bepler T, Kelley K, Noble AJ, Berger B: **Topaz-Denoise: general deep denoising models for cryoEM and cryoET**. *Nat Commun* 2020, **11**:5208.
5. Lehtinen J, Munkberg J, Hasselgren J, Laine S, Karras T, Aittala M, Aila T: **Noise2Noise: learning image restoration without clean data**. *arXiv [cs.CV]*, 2018. <https://doi.org/10.48550/arXiv.1803.04189>.
6. Costa-Filho JI, Theveny L, de Sautu M, Kirchhausen T: **Cryo-Samba: self-supervised deep volumetric denoising for cryo-electron tomography data**. *J Struct Biol* 2025, **217**, <https://doi.org/10.1016/j.jsb.2024.108163>.
7. Liu Y-T, Zhang H, Wang H, Tao C-L, Bi G-Q, Zhou ZH: **Isotropic reconstruction for electron tomography with deep learning**. *Nat Commun* 2022, **13**:6482.
8. Wiedemann S, Heckel R: **A deep learning method for simultaneous denoising and missing wedge reconstruction in cryogenic electron tomography**. 2024.
9. Majtner T, Kreysing JP, Tuijtel MW, Cruz-León S, Liu J, Hummer G, Beck M, Turoňová B: **cryoTIGER: deep-learning based tilt interpolation generator for enhanced reconstruction in cryo electron tomography**. *bioRxiv* 2024, <https://doi.org/10.1101/2024.12.17.628939>. 2024.2012.2017.628939.
- This preprint presents cryoTIGER, a deep learning-based workflow for calculating and correcting for information lost due to incomplete angular sampling during tilt series data collection.
10. Chen M, Dai W, Sun SY, Jonasch D, He CY, Schmid MF, Chiu W, Ludtke SJ: **Convolutional neural networks for automated annotation of cellular cryo-electron tomograms**. *Nat Methods* 2017, **14**:983–985.
11. Moebel E, Martinez-Sanchez A, Lamm L, Righetto RD, Wietrzynski W, Albert S, Larivière D, Fourmentin E, Pfeffer S, Ortiz J, et al.: **Deep learning improves macromolecule identification in 3D cellular cryo-electron tomograms**. *Nat Methods* 2021, **18**:1386–1394.
12. Heebner JE, Purnell C, Hylton RK, Marsh M, Grillo MA, Swulius MT: **Deep learning-based segmentation of cryo-electron tomograms**. *J Vis Exp* 2022, <https://doi.org/10.3791/64435>.
13. de Teresa-Trueba I, Goetz SK, Mattausch A, Stojanovska F, Zimmerli CE, Toro-Nahuelpan M, Cheng DWC, Tollervey F, Pape C, Beck M, et al.: **Convolutional networks for supervised mining of molecular patterns within cellular context**. *Nat Methods* 2023, **20**:284–294.
- This manuscript presents DeePiCt, one of the first generalizable segmentation tools to offer a pretrained model for the semantic segmentation of macromolecules, organellar membranes, and filaments from cryo-ET data, eliminating the need for substantial user input for training.
14. Martinez-Sanchez A, Lamm L, Jasnin M, Phelippeau H: **Simulating the cellular context in synthetic datasets for cryo-electron tomography**. *IEEE Trans Med Imag* 2024, **43**: 3742–3754.
- This publication presents a Python package that generates simulated cryo-ET datasets by incorporating models of low-order molecular structures, such as macromolecule clusters, membranes, and cytoskeletal filaments, to create training datasets for machine learning algorithms.
15. Purnell C, Heebner J, Nguyen L, Swulius MT, Hylton R, Kabonick S, Grillo M, Grillo S, Grigoryev S, Heberle FA, et al.: **Training generalized segmentation networks with real and synthetic cryo-ET data**. *bioRxiv* 2025, <https://doi.org/10.1101/2025.01.31.635598>. 2025.2001.2031.635598.
- This preprint presents cryo-TomoSim (CTS), a MATLAB-based software tool that generates simulated cryo-ET datasets from PDB models to overcome the lack of ground truth data for training machine learning models in denoising and semantic segmentation.
16. Harar P, Herrmann L, Grohs P, Haselbach D: **FakET: simulating cryo-electron tomograms with neural style transfer**. *Structure* 2025, **33**:820–827.e824.
17. Martinez-Sanchez A, Garcia I, Asano S, Lucic V, Fernandez J-J: **Robust membrane detection based on tensor voting for electron tomography**. *J Struct Biol* 2014, **186**:49–61.
18. Stalling D, Westerhoff M, Hege H-C: **38 - amira: a highly interactive system for visual data analysis**. In *Visualization handbook*. Edited by Hansen CD, Johnson CR, Butterworth-Heinemann; 2005:749–767, <https://doi.org/10.1016/B978-012387582-2/50040-X>.
19. Siggel M, Jensen RK, Maurer VJ, Mahamid J, Kosinski J: **ColabSeg: an interactive tool for editing, processing, and**

- visualizing membrane segmentations from cryo-ET data.** *J Struct Biol* 2024, **216**, 108067.
20. Lamm L, Zufferey S, Righetto RD, Wietrzynski W, Yamauchi KA, Burt A, Liu Y, Zhang H, Martinez-Sanchez A, Ziegler S, *et al.*: **MemBrain v2: an end-to-end tool for the analysis of membranes in cryo-electron tomography.** *bioRxiv* 2024, <https://doi.org/10.1101/2024.01.05.574336>. 2024.2001.2005.574336.

This preprint introduces MemBrain V2, a deep learning-enabled program for comprehensive analysis of membranes visible in cryo-ET, including automated membrane-centric segmentation, particle picking, and morphometrics.

 21. Khosrozadeh A, Seeger R, Witz G, Radecke J, Sørensen JB, Zuber B: **CryoVesNet: a dedicated framework for synaptic vesicle segmentation in cryo-electron tomograms.** *JCB (J Cell Biol)* 2024, **224**, e202402169.

This manuscript presents CryoVesNet, a workflow designed specifically for the automatic segmentation of spherical vesicles, such as synaptic vesicles, from tomographic data.

 22. Salfer M, Collado JF, Baumeister W, Fernández-Busnadiego R, Martínez-Sánchez A: **Reliable estimation of membrane curvature for cryo-electron tomography.** *PLoS Comput Biol* 2020, **16**, e1007962.
 23. Barad BA, Medina M, Fuentes D, Wiseman RL, Grotjahn DA: **Quantifying organellar ultrastructure in cryo-electron tomography using a surface morphometrics pipeline.** *J Cell Biol* 2023, **222**.

We present a surface morphometrics pipeline, which converts voxel segmentations of diverse cellular membranes into surface mesh reconstructions and provides a comprehensive of tools for quantifying membrane architecture through morphometric analysis.

 24. Rigort A, Günther D, Hegerl R, Baum D, Weber B, Prohaska S, Medalia O, Baumeister W, Hege HC: **Automated segmentation of electron tomograms for a quantitative description of actin filament networks.** *J Struct Biol* 2012, **177**:135–144.
 25. Sazzed S, Scheible P, He J, Wriggers W: **Untangling irregular actin cytoskeleton architectures in tomograms of the cell with struwel tracer.** *Int J Mol Sci* 2023, **24**.
 26. Castaño-Díez D, Kudryashev M, Stahlberg H: **Dynamo Catalogue: geometrical tools and data management for particle picking in subtomogram averaging of cryo-electron tomograms.** *J Struct Biol* 2017, **197**:135–144.
 27. Hylton RK, Heebner JE, Grillo MA, Swilius MT: **Cofilactin filaments regulate filopodial structure and dynamics in neuronal growth cones.** *Nat Commun* 2022, **13**:2439.
 28. Tollervy F, Rios MU, Zagorij E, Woodruff JB, Mahamid J: **Molecular architectures of centrosomes in C. elegans embryos visualized by cryo-electron tomography.** *Dev Cell* 2024, <https://doi.org/10.1016/j.devcel.2024.12.002>.
 29. Zhang X, Mahamid J: **Protocol for subtomogram averaging of helical filaments in cryo-electron tomography.** *STAR Protoc* 2024, **5**, 103272.
 30. Navarro PP, Stahlberg H, Castaño-Díez D: **Protocols for subtomogram averaging of membrane proteins in the Dynamo software package.** *Front Mol Biosci* 2018, **5**:82.
 31. Basanta B, Chowdhury S, Lander GC, Grotjahn DA: **A guided approach for subtomogram averaging of challenging macromolecular assemblies.** *J Struct Biol X* 2020, **4**, 100041.
 32. Watanabe R, Zyla D, Parekh D, Hong C, Jones Y, Schendel SL, Wan W, Castillon G, Saphire EO: **Intracellular Ebola virus nucleocapsid assembly revealed by in situ cryo-electron tomography.** *Cell* 2024, **187**:5587–5603.e5519.
 33. Burt A, Gaifas L, Dendooven T, Gutsche I: **A flexible framework for multi-particle refinement in cryo-electron tomography.** *PLoS Biol* 2021, **19**, e3001319.
 34. Held RG, Liang J, Esquivies L, Khan YA, Wang C, Azubel M, Brunger AT: **In-Situ structure and topography of AMPA receptor scaffolding complexes visualized by CryoET.** *bioRxiv* 2024, <https://doi.org/10.1101/2024.10.19.619226>.
 35. Noble AJ, de Marco A: **Cryo-focused ion beam for in situ structural biology: state of the art, challenges, and perspectives.** *Curr Opin Struct Biol* 2024, **87**, 102864.
 36. Mageswaran SK, Grotjahn DA, Zeng X, Barad BA, Medina M, Hoang MH, Dobro MJ, Chang YW, Xu M, Yang WY, *et al.*: **Nanoscale details of mitochondrial constriction revealed by cryoelectron tomography.** *Biophys J* 2023, **122**:3768–3782.
 37. Kirchweber P, Wolf SG, Varsano N, Dadosh T, Resch GP, Elbaum M: **Snapshots of mitochondrial fission imaged by cryo-scanning transmission electron tomography.** *J Cell Sci* 2025, **138**, <https://doi.org/10.1242/jcs.263639>.
 38. Wang R, Lei H, Wang H, Qi L, Liu Y, Liu Y, Shi Y, Chen J, Shen QT: **Dysregulated inter-mitochondrial crosstalk in glioblastoma cells revealed by in situ cryo-electron tomography.** *Proc Natl Acad Sci U S A* 2024, **121**, e2311160121.
 39. Fry MY, Navarro PP, Hakim P, Ananda VY, Qin X, Landoni JC, Rath S, Inde Z, Lugo CM, Luce BE, *et al.*: **In situ architecture of Opa1-dependent mitochondrial cristae remodeling.** *EMBO J* 2024, **43**:391–413. 413.
 40. Nakamura K, Aoyama-Ishiwatari S, Nagao T, Paaran M, Obara CJ, Sakurai-Saito Y, Johnston J, Du Y, Suga S, Tsuboi M, *et al.*: **PDZD8-FKBP8 tethering complex at ER-mitochondria contact sites regulates mitochondrial complexity.** *Nat Commun* 2025, <https://doi.org/10.1038/s41467-025-58538-3>.
 41. Gong B, Johnston JD, Thiemiecke A, de Marco A, Meyer T: **Endoplasmic reticulum–plasma membrane contact gradients direct cell migration.** *Nature* 2024, **631**:415–423.
 42. Li M, Tripathi-Giesgen I, Schulman BA, Baumeister W, Wilfling F: **In situ snapshots along a mammalian selective autophagy pathway.** *Proc Natl Acad Sci U S A* 2023, **120**, e2221712120.
 43. Kucińska MK, Fedry J, Galli C, Morone D, Raimondi A, Soldà T, Förster F, Molinari M: **TMX4-driven LINC complex disassembly and asymmetric autophagy of the nuclear envelope upon acute ER stress.** *Nat Commun* 2023, **14**:3497.
 44. Santos Ád, Knowles O, Dendooven T, Hale T, Hale VL, Burt A, Kolata P, Cannone G, Bellini D, Barford D, *et al.*: **Human spermatogenesis leads to a reduced nuclear pore structure and function.** *bioRxiv* 2024, <https://doi.org/10.1101/2024.10.30.620797>. 2024.2010.2030.620797.
 45. Bäuerlein FJB, Renner M, Chami DE, Lehnart SE, Pastor-Pareja JC, Fernández-Busnadiego R: **Cryo-electron tomography of large biological specimens vitrified by plunge freezing.** *bioRxiv* 2023, <https://doi.org/10.1101/2021.04.14.437159>. 2021.2004.2014.437159.
 46. Dahmane S, Schexnaydre E, Zhang J, Rosendal E, Chotiwan N, Kumari Singh B, Yau WL, Lundmark R, Barad B, Grotjahn DA, *et al.*: **Cryo-electron tomography reveals coupled flavivirus replication, budding and maturation.** *bioRxiv* 2024, <https://doi.org/10.1101/2024.10.13.618056>.
 47. Dimchev G, Amiri B, Fäßler F, Falcke M, Schur FK: **Computational toolbox for ultrastructural quantitative analysis of filament networks in cryo-ET data.** *J Struct Biol* 2021, **213**, 107808.
 48. Li W, Li A, Yu B, Zhang X, Liu X, White KL, Stevens RC, Baumeister W, Sali A, Jasnin M, *et al.*: **In situ structure of actin remodeling during glucose-stimulated insulin secretion using cryo-electron tomography.** *Nat Commun* 2024, **15**:1311.
 49. Atherton J, Stouffer M, Francis F, Moores CA: **Visualising the cytoskeletal machinery in neuronal growth cones using cryo-electron tomography.** *J Cell Sci* 2022, **135**.
 50. Lembo S, Strauss L, Cheng D, Vermeil J, Siggel M, Toro-Nahuelpan M, Chan CJ, Kosinski J, Piel M, Du Roure O, *et al.*: **The distance between the plasma membrane and the actomyosin cortex acts as a nanogate to control cell surface mechanics.** *bioRxiv* 2023, <https://doi.org/10.1101/2023.01.31.526409>. 2023.2001.2031.526409.
 51. Yamauchi KA, Lamm L, Gaifas L, Righetto RD, Litvinov D, Engel BD, Harrington K: **Surforama: interactive exploration of volumetric data by leveraging 3D surfaces.** *bioRxiv* 2024, <https://doi.org/10.1101/2024.05.30.596601>. 2024.2005.2030.596601.

This preprint presents Surforama, a Napari plugin that renders local protein densities on surface mesh reconstructions, enabling the

interactive visualization and particle picking of membrane-associated macromolecules in tomograms.

52. Papantoniou C, Laugks U, Betzin J, Capitanio C, Ferrero JJ, Sánchez-Prieto J, Schoch S, Brose N, Baumeister W, Cooper BH, *et al.*: **Munc13- and SNAP25-dependent molecular bridges play a key role in synaptic vesicle priming.** *Sci Adv* 2023, **9**, ead6222.
 53. Radecke J, Seeger R, Kádková A, Laugks U, Khosrozadeh A, Goldie KN, Lúčić V, Sørensen JB, Zuber B: **Morphofunctional changes at the active zone during synaptic vesicle exocytosis.** *EMBO Rep* 2023, **24**, e55719.
 54. Held RG, Liang J, Brunger AT: **Nanoscale architecture of synaptic vesicles and scaffolding complexes revealed by cryo-electron tomography.** *Proc Natl Acad Sci U S A* 2024, **121**, e2403136121.
 55. Glushkova D, Böhm S, Beck M: **In situ evidence for systematic membrane thickness variation across cellular organelles.** *bioRxiv* 2025, <https://doi.org/10.1101/2025.03.13.642912>. 2025.2003.2013.642912.
 56. Medina M, Chang Y-T, Rahmani H, Fuentes D, Barad BA, Grotjahn DA: **Surface morphometrics reveals local membrane thickness variation in organellar subcompartments.** *bioRxiv* 2025, <https://doi.org/10.1101/2025.04.30.651574>. 2025.2004.2030.651574.
 57. Chang YT, Barad BA, Rahmani H, Zid BM, Grotjahn DA: **Cytoplasmic ribosomes on mitochondria alter the local membrane environment for protein import.** *J Cell Biol* 2025, **224**, <https://doi.org/10.1083/jcb.202407110>.
- In this article, we used the surface morphometrics pipeline to identify a subset of ribosomes optimally positioned for import on the mitochondrial membrane. We also developed a patch-based analysis to detect local changes in membrane ultrastructure in regions associated with import-oriented ribosomes.
58. Gemin O, Gluc M, Rosa H, Purdy M, Niemann M, Peskova Y, Mattei S, Jomaa A: **Ribosomes hibernate on mitochondria during cellular stress.** *Nat Commun* 2024, **15**:8666.
 59. Martinez M, Mageswaran SK, Guérin A, Chen WD, Thompson CP, Chavin S, Soldati-Favre D, Striepen B, Chang Y-W: **Origin and arrangement of actin filaments for gliding motility in apicomplexan parasites revealed by cryo-electron tomography.** *Nat Commun* 2023, **14**:4800.
 60. Li Z, Du W, Yang J, Lai DH, Lun ZR, Guo Q: **Cryo-electron tomography of toxoplasma gondii indicates that the conoid fiber may be derived from microtubules.** *Adv Sci (Weinh)* 2023, **10**, e2206595.
 61. Jentoft IMA, Bäuerlein FJB, Welp LM, Cooper BH, Petrovic A, So C, Penir SM, Politi AZ, Horokhovskiy Y, Takala I, *et al.*: **Mammalian oocytes store proteins for the early embryo on cytoplasmic lattices.** *Cell* 2023, **186**:5308–5327.e5325.
 62. Gaifas L, Kirchner MA, Timmins J, Gutsche I: **Blik is an extensible 3D visualisation tool for the annotation and analysis of cryo-electron tomography data.** *PLoS Biol* 2024, **22**, e3002447.
- This manuscript presents Blik, a Napari plugin that enables the simultaneous visualization of tomograms, particle picks, and segmentations. This software also features tooling for membrane surface and filament model-based segmentation and particle picking.
63. Johnston B, Elferich J, Davidson RB, Zhuang Y, Yao Y, Tubiana T, Kunzmann P, Rich Laprevote O, TheJeran, *et al.*: **BradyAJohnston/MolecularNodes: v4.2.10 for blender 4.2+.** In *Zenodo*. edn v4.2.10 2024, <https://doi.org/10.5281/zenodo.14534390>.
 64. Ermel UH, Arghittu SM, Frangakis AS: **ArtiaX: an electron tomography toolbox for the interactive handling of sub-tomograms in UCSF ChimeraX.** *Protein Sci* 2022, **31**, e4472.
 65. Ahrens J, Geveci B, Law C: **ParaView: an end-user tool for large data visualization.** *Visualization Handbook* 2005.
 66. Sullivan CB, Kaszynski A: **PyVista: 3D plotting and mesh analysis through a streamlined interface for the Visualization Toolkit (VTK).** *J Open Source Softw* 2019, **4**:1450.
 67. Last MGF, Abendstein L, Voortman LM, Sharp TH. In *Ais: streamlining segmentation of cryo-electron tomography datasets*. eLife Sciences Publications, Ltd; 2024, <https://doi.org/10.7554/elife.98552.2>.
- This manuscript presents Ais, a segmentation package for automated, large-scale segmentation of cryo-ET data. Ais was recently applied to segment a dataset of over 1800 tomograms of cryo-focused ion beam (cryo-FIB) milled *Chlamydomonas reinhardtii* tomograms in the CryoET data portal.
68. Kiewisz R, Fabig G, Conway W, Johnston J, Kostyuchenko V, Barinka C, Clarke OB, Magaj M, Yazdkhasti H, Vallese F, *et al.*: **Accurate and fast segmentation of filaments and membranes in micrographs and tomograms with TARDIS.** *bioRxiv* 2024, <https://doi.org/10.1101/2024.12.19.629196>. 2024.2012.2019.629196.
- This manuscript presents TARDIS, a segmentation package for automated, large-scale segmentation of cryo-ET data. TARDIS was recently applied to segment a dataset of over 1300 tomograms of cryo-focused ion beam (cryo-FIB) milled *Chlamydomonas reinhardtii* tomograms in the CryoET data portal.
69. Ermel U, Cheng A, Ni JX, Gadling J, Venkatakrishnan M, Evans K, Asuncion J, Sweet A, Pourroy J, Wang ZS, *et al.*: **A data portal for providing standardized annotations for cryo-electron tomography.** *Nat Methods* 2024, **21**:2200–2202.
- This manuscript presents the cryoET Data Portal, a data repository explicitly designed for depositing annotated cryo-electron tomography datasets.
70. Wan W: **A case for community metadata standards in cryo-electron tomography.** *Emerging Topics in Life Sciences* 2025, <https://doi.org/10.1042/etls20240013>.